

A longitudinal flight control law based on robust MPC and \mathcal{H}_2 methods to accommodate sensor loss in the RECONFIGURE benchmark^{*}

E. N. Hartley^{*} J. M. Maciejowski^{*}

^{*} *University of Cambridge, Department of Engineering, Cambridge, CB2 1PZ, United Kingdom. (e-mail: {enh20,jmm}@eng.cam.ac.uk).*

Abstract: The feedback gains in state-of-the-art flight control laws for commercial aircraft are scheduled as a function of values such as airspeed, mass, and centre of gravity. If estimates of these are lost due to multiple simultaneous sensor failures, it is necessary for the pilot to either directly command control surface positions, or to revert to an alternative control law. This work develops a robust backup load-factor tracking control law, that does not depend on these parameters, based on application of theory from robust MPC and \mathcal{H}_2 control. First the methods are applied with loss only of airdata, and subsequently also with loss of mass and CoG estimates. Local linear analysis indicates satisfactory performance over a wide range of operating points. Finally, the resulting control laws are demonstrated on the nonlinear RECONFIGURE benchmark, which is derived from Airbus's high fidelity, industrially-validated simulator, OSMA.

Keywords: Optimal control, Robust control, Aircraft control, Fault-tolerant control

1. INTRODUCTION

Automatic control systems are integral to the operation of modern civil airliners (Favre, 1994), reducing the pilot's workload through stability augmentation and providing a homogeneous response to commands through the whole flight envelope. The open-loop response of the aircraft varies considerably, and when a linear feedback control law is used, it is usual to schedule its parameters based on the flight point. For example when controlling the longitudinal short-period mode, load factor (n_z) and pitch rate (q) are fed-back, but the control law parameters are scheduled as a function of a combination of airspeed, altitude, mach number, mass and centre-of-gravity of the aircraft. Each parameter used must therefore be measured or estimated.

Unfortunately, faults can occur. Hardware redundancy is the typical mitigating measure (Brière et al., 1995; Goupil, 2011). To achieve robustness to sensor failure, multiple (possibly dissimilar) sensors can be implemented and a "voting" mechanism employed to detect and compensate for a pre-determined number of failures Goupil (2011). Analytical redundancy (where multiple signals are combined to reconstruct an estimate of a parameter without explicitly measuring it) can also be exploited through soft sensor design, providing additional fault-tolerance without the burden of additional physical hardware. However when too many simultaneous sensor faults occur, the signals must be treated as polluted and ignored.

This paper considers first the case where airspeed data is lost, for example due to multiple simultaneous faults on

^{*} The research leading to these results has received funding from the European Union Seventh Framework Programme FP7/2007-2013 under grant agreement number 314 544, project "RECONFIGURE".

pitot tubes and angle-of-attack sensors (so AoA cannot be used to estimate airspeed). In this situation, one recourse is to switch to a direct control law, where elevator deflection is commanded instead. However, it would be desirable to maintain a load-factor control law with reasonable robustness and handling qualities, so as to limit the inevitable additional workload falling on the pilot. Stable operation is subsequently demonstrated where estimates of mass, centre of gravity are also lost.

Recently, Puyou and Ezerzere (2012) achieved a similar objective, applying non-smooth optimisation to obtain a fixed-complexity controller robust to loss of mass and centre of gravity estimates. The remaining scheduling information was introduced through an inner-loop nonlinear dynamic inversion (NDI) controller due to difficulties interpolating dynamic systems. Similarly, Varga et al. (2014) proposes a non-scheduled backup C^* control law, tuned using multi-objective optimisation. The present work demonstrates an alternative method for maintaining a load factor control law using a robust discrete-time control technique. The controller is designed using local linearisations of the longitudinal dynamics of an Airbus A380, and then tested in an industrial high-fidelity nonlinear simulator provided by Airbus for use in the RECONFIGURE project, based on an evolution of OSMA (Outil de Simulation des Mouvements Avion, Favre (1994)).

This paper has the following structure. Section 2 outlines the control problem. Section 3 describes the theoretical tools which will be applied. Section 4 describes the tuning method and linear analysis of the resulting control law. Section 5 then demonstrates the control laws in a high fidelity nonlinear simulation, and Section 6 concludes. The key purpose of this paper is not the development of new

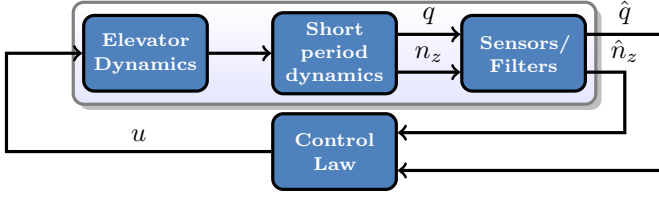


Fig. 1. Schematic of control design setup

theory, but an approach to address the requirements of a challenging industrially-motivated application.

2. CONTROL PROBLEM

Airbus has provided the RECONFIGURE consortium with linearisations of the longitudinal dynamics of an Airbus A380 in straight-and-level flight at 214 different flight points covering an envelope of altitudes, airspeeds, masses and centre-of-gravity (CoG), as well as simplified linear sensor, filter and actuator models. We consider a setup where all elevators act in common mode, and neglect the trimmable-horizontal-stabiliser (THS), which in any case can only control at much lower frequency ranges than those considered. A sampling period $T_s = 0.04$ s is used.

The objective is to control only the short-period dynamics (leaving the pilot or an autopilot control law to control the phugoid mode). Classically the short-period dynamics are modelled with the pitch rate q and angle-of-attack α as states, with q , α and vertical “load factor” n_z as outputs. Usually, α is not available at sufficiently high bandwidth to be used for the innermost control loop, so q and n_z are used as feedback variables. The control input is the elevator deflection (multiple elevators operating in common mode). For design purposes, the short-period model at each flight point is augmented with a first-order-plus delay actuator model for the elevator and first-order low-pass linear sensor models on q and n_z , followed by a first-order low-pass filter yielding estimates \hat{q} and \hat{n}_z of the true values (Figure 1). These approximate the higher order “true” filters, which also include notch filters to attenuate certain structural modes, and the assumption is made that the existing filters are unalterable.

Let x denote the combined state-vector of the actuator dynamics, short-period mode and sensors/filters and y denote that measured output $[\hat{q}, \hat{n}_z]^T$. The short-period dynamics vary with the current airspeed, altitude, CoG, and mass. We will denote these parameters that determine the flight point as θ . The augmented linearised plant model at a given flight point θ sampled at time step k , with period T_s can be described by the parameterised linear difference equations:

$$x(k+1) = A(\theta)x(k) + B(\theta)u(k) \quad (1a)$$

$$y(k) = C(\theta)x(k) + D(\theta)u(k). \quad (1b)$$

Delays in the model mean this is strictly proper, i.e. $D = 0$.

The specification for the RECONFIGURE project (Goupil et al., 2014) states that the closed-loop response should have the following time-domain characteristics. First, the response to a step change in commanded n_z should be “substantially finished” within 6 s. The corresponding pitch rate q should not overshoot its steady state value by more than 30% and the load factor should not overshoot its

setpoint by more than 10%, and the “control anticipation parameter” (CAP) should be “homogeneous” throughout the flight envelope. In addition it is desirable to have a local 60° phase margin and a 6 dB gain margin at the linear design points, although in degraded conditions, it may not be possible to achieve all of these simultaneously on top of the nominal design uncertainty.

3. THEORETICAL GROUNDING

Let $\mathcal{I} \triangleq \{1, \dots, 214\}$ be an index for the 214 design points, and θ_i , for $i \in \mathcal{I}$ denote the flight parameters for the i th flight point. Define subsets of the flight points $\mathcal{J}_j \subseteq \mathcal{I}$, $j = 0, \dots, j_{\max}$, as “flight groups” such that $\mathcal{J}_m \cap \mathcal{J}_n = \emptyset$, $\forall m \neq n$, and let θ_{ji} denote the parameters of the flight point indexed by the i th element of \mathcal{J}_j . The design objective can be posed as the finding j_{\max} control laws $\kappa_j(z)$ that each stabilise all flight points in \mathcal{J}_j , with satisfactory tracking performance. We assume that parameters vary slowly in comparison to the controlled dynamics and can be locally approximated as time-invariant.

3.1 Output-feedback transformation

This is an *output feedback* control problem. For an observer-based control law, a nominal plant model would need to be chosen (the choice of which is not obvious). Moreover, since non-zero setpoints are to be tracked, the usual assumption that observer error converges to zero is invalid. On the other hand, a static, or arbitrary order feedback law might be difficult to tune. The alternative used here is to transform (1) for each flight point into a non-minimal input-output form whose “state” is a finite time history of inputs and outputs. The “state-observer” for this is then simply a set of shift registers. This form was commonly used in legacy implementations of MPC for SISO systems (Maciejowski, 2002), and has also been recently highlighted in Granado et al. (2005); Ding and Zou (2014) for applying state-feedback control techniques for uncertain systems in an output-feedback setting. This form also means that the controller state has the same physical interpretation at all flight points, and thus interpolating a feedback gain between flight points using the remaining available parameters is a possible strategy. The present application has the complication of multiple measured outputs but the same principles hold. This is not quite as simple as using MATLAB’s “ss2tf” command and extracting the coefficients. The following proposes a systematic method to compute such a form.

Assume that the plant (1) is m -step observable, and that the number of states in (1) is a whole multiple of m . Define the augmented state $\tilde{x}(k) = [\mathbf{u}(k)^T \mathbf{y}(k)^T]^T$ where $\mathbf{u}(k) = [u(k-m) \dots u(k-1)]^T$ and $\mathbf{y}(k) = [y(k-m)^T \dots y(k-1)^T]^T$. Letting dependency on θ be implicit (and approximated as time-invariant), define

$$\Phi = \begin{bmatrix} C \\ \vdots \\ CA^{m-2} \\ CA^{m-1} \end{bmatrix}, \quad \Gamma = \begin{bmatrix} D & & & \\ \cdots & \ddots & & \\ \cdots & CB & D & \\ \cdots & CAB & CB & D \end{bmatrix} \quad (2)$$

and

$$\Psi = [CA^{m-1}B \dots CA^2B \quad CAB \quad CB]. \quad (3)$$

Theorem 1. $y(k) = (\Psi - CA^m\Phi^{-1}\Gamma)\mathbf{u}(k) + CA^m\Phi^{-1}\mathbf{y}(k) + Du(k)$.

Proof. At a given flight point, it holds that

$$\mathbf{y}(k) = \Phi x(k-m) + \Gamma\mathbf{u}(k). \quad (4)$$

Since we have assumed the plant to be m -step observable,

$$\begin{aligned} x(k-m) &= \Phi^{-1}(\mathbf{y}(k) - \Gamma\mathbf{u}(k)) \\ y(k) &= CA^m x(k-m) + \Gamma\mathbf{u}(k) + Du(k) \\ &= CA^m\Phi^{-1}(\mathbf{y}(k) - \Gamma\mathbf{u}(k)) + \Psi\mathbf{u}(k) + Du(k) \\ &= (\Psi - CA^m\Phi^{-1}\Gamma)\mathbf{u}(k) + CA^m\Phi^{-1}\mathbf{y}(k) + Du(k). \end{aligned}$$

Thus, the non-minimal state-space system is:

$$\begin{aligned} \tilde{x}(k+1) &= \begin{bmatrix} 0 & I_{(m-1)n_u} & 0 \\ 0 & 0 & 0 \\ 0 & 0 & 0 \\ \Psi - CA^m\Phi^{-1}\Gamma & CA^m\Phi^{-1} & 0 \end{bmatrix} \tilde{x}(k) + \begin{bmatrix} 0 \\ I \\ 0 \\ D \end{bmatrix} u(k) \\ y(k) &= [(\Psi - CA^m\Phi^{-1}\Gamma) \quad CA^m\Phi^{-1}] \tilde{x}(k) + Du(k). \end{aligned} \quad (5)$$

This is generalised to systems with a higher observability index and systems where the state dimension is not an integer multiple of the outputs by increasing the length of the time history of inputs and outputs, m until Φ is of full row rank, and using the Moore-Penrose Pseudo-inverse, Φ^+ instead of Φ^{-1} . We will denote the nonminimal system realisation with the matrices $\tilde{A}(\theta)$, $\tilde{B}(\theta)$, $\tilde{C}(\theta)$, $\tilde{D}(\theta)$.

3.2 Robust control theory

One way to design a control law that is robust to large degrees of parametric uncertainty is to choose a nominal plant model and then characterise uncertainty around it. However, such a choice is not obvious. Instead, the tool applied here is based on robust MPC theory and \mathcal{H}_2 control theory. Kothare et al. (1996) proposed a method based on linear matrix inequalities (LMIs) to simultaneously stabilise a set of linear plants. At each time step, an optimisation is solved to find a controller of form $u(k) = K(x(k))x(k)$ that minimises an upper bound on a quadratic cost function over an infinite horizon from the current state. Input and output constraints can also be accommodated, conservatively. Cuzzola et al. (2002) suggests a less conservative method based on multiple Lyapunov functions (de Oliveira et al., 1999; De Oliveira et al., 2002). This is prohibitively computationally demanding for the present application. However, Wan and Kothare (2002) proposes an offline method, based on interpolation of gains computed at judiciously selected states based on set membership conditions. The present work does not consider constraints: the tracking nature of the problem adds complications with constraints and large amounts of plant/model mismatch. For tracking, we will follow the classical technique of augmenting the plant with an integrator of the error between the load factor to be tracked and the reference. Let $H = [0, 1]$, and $A_i = 1$, $B_i = T_s$ be the state space matrices of the integrator, then the augmented system is

$$\underbrace{\begin{bmatrix} e(k+1) \\ \tilde{x}(k+1) \end{bmatrix}}_{\tilde{x}(k+1)} = \underbrace{\begin{bmatrix} A_i & -B_i H \tilde{C}(\theta) \\ 0 & \tilde{A}(\theta) \end{bmatrix}}_{\tilde{A}(\theta)} \underbrace{\begin{bmatrix} e(k) \\ \tilde{x}(k) \end{bmatrix}}_{\tilde{x}(k)} + \underbrace{\begin{bmatrix} -B_i H \tilde{D}(\theta) \\ \tilde{B}(\theta) \end{bmatrix}}_{\tilde{B}(\theta)} u(k) + \underbrace{\begin{bmatrix} B_i \\ 0 \end{bmatrix}}_{B_r} r(k). \quad (6)$$

The objective reduces now to synthesising control gains K_j that stabilise our integrator-augmented short-period-plus-elevator-plus-sensor input-output composite models.

The control synthesis objective is, for each group \mathcal{J}_j , to minimise an upper bound on

$$\min_{K_j} \max_{\theta_{ji} \in \mathcal{J}_j} \sum_{k=0}^{\infty} \bar{x}(k)^T (Q + K_j^T R K_j + S K_j + K_j^T S^T) \bar{x}(k). \quad (7)$$

The cross term is helpful for this application.

Lemma 2. $K^T R K + S K + K^T S^T = (K^T + S R^{-1}) R (K + R^{-1} S^T) - S R^{-1} S^T$

Proof. By expansion.

With this, we can apply the result of Cuzzola et al. (2002) for a general quadratic cost function:

Theorem 3. $\sum_{k=0}^{\infty} \bar{x}(k)^T (Q + K_j^T R K_j + S K_j + K_j^T S^T) \bar{x}(k) \leq \gamma_j$ if $Y_j = K_j G_j$ and for all $\theta_{ji} \in \mathcal{J}_j$,

$$\begin{bmatrix} G_j + G_j^T - X_{ji} & * & * & * \\ (\tilde{A}(\theta_{ji}) + \tilde{B}(\theta_{ji})) Y & X_{ji} & 0 & 0 \\ (Q - S R^{-1} S^T)^{1/2} G_j & 0 & \gamma_j I & 0 \\ R^{1/2} (Y_j + R^{-1} S^T G_j) & 0 & 0 & \gamma_j I \end{bmatrix} \geq 0 \quad (8a)$$

$$\begin{bmatrix} 1 & \bar{x}(k)^T \\ \bar{x}(k) & X_{ji} \end{bmatrix} \geq 0 \quad (8b)$$

Corollary 4. The control law $u(k) = Y_j G_j^{-1} \bar{x}(k) = K_j \bar{x}(k)$, obtained by solution of

$$\min_{\gamma, G_j, X_{ji}, Y_j} \gamma_j \text{ subject to (8)} \quad (9)$$

minimises an upper bound on the cost function (7).

Solving (9) online for each new $\bar{x}(k)$ is not appropriate for an aircraft inner control loop where the sampling period is in the order of tens of milliseconds due to the complexity of the required software, the required solution time, and the limited computational hardware. Instead, following the lead of Wan and Kothare (2002) the problem is solved offline for a fixed value of $\bar{x}(k) = \bar{x}_0$ and the resulting control gain used for all $\bar{x}(k)$ given the relevant flight parameters. Thus, the final implementation used here is not ‘‘MPC’’ in the conventional sense, and can rather be interpreted as a form of \mathcal{H}_2 controller.

The dynamic output feedback control law $\kappa_j(z)$ is parameterised by a dynamic, but fixed component $G_K(z)$ and a flight-group dependent gain K_j . Letting A_s , B_{su} , and B_{sy} denote the shift registers formed as in (5), and $\hat{\tilde{x}}$ denote the estimate of $\tilde{x}(k)$ contained therein, the fixed component $G_K(z)$ can be described by the system:

$$\begin{bmatrix} e(k+1) \\ \hat{\tilde{x}}(k+1) \\ e(k) \\ \hat{\tilde{x}}(k) \\ u(k) \end{bmatrix} = \begin{bmatrix} A_i & 0 & 0 & -B_i H & B_i \\ 0 & A_s & B_{su} & B_{sy} & 0 \\ I & 0 & 0 & 0 & 0 \\ 0 & I & 0 & 0 & 0 \\ 0 & 0 & I & 0 & 0 \end{bmatrix} \begin{bmatrix} e(k) \\ \hat{\tilde{x}}(k) \\ u(k) \\ y(k) \\ r(k) \end{bmatrix}. \quad (10)$$

The static component is K_j , and the dynamic controller can be described by the upper linear fractional transform

$$\kappa_j(z) = \mathcal{F}_u(G_K(z), K_j), \quad (11)$$

i.e., the control input is computed by multiplying the integrator state and the shift register state by the gain.

4. LINEAR DESIGN

For synthesis, we model the actuator dynamics with the discrete transfer function $0.3297/(z^2 - 0.6703z)$. The pitch rate

sensor and filter are modelled as $(0.118z + 0.06885)/(z^3 - 1.01z^2 + 0.1967z)$ and the load factor sensor and filter are modelled as $(0.1417z + 0.08081)/(z^3 - 0.9615z^2 + 0.184z)$. These constitute a low-order approximation of the real ones. The short-period dynamic model considers only the states α , and q , a single lumped elevator input and outputs q and n_z .

For tuning, we define a performance output $z(k) = [e(k), q(k-1), n_z(k-1), \Delta q(k-1), \Delta n_z(k-1), u(k), \Delta u(k)]^T$, where $\Delta u(k) = u(k) - u(k-1)$, and $z(k) = C_p(\theta)\bar{x}(k) + D_p(\theta)u(k)$, and the objective is to thus, minimise an upper bound on $\sum_{k=0}^{\infty} z(k)^T Q z(k)$ over all $\theta_{ji} \in \mathcal{J}_j$, where we define Q with tuning weights on the diagonal as

$$Q \triangleq \text{diag}\{1, Q_q, Q_{n_z}, Q_{\Delta q}, Q_{\Delta n_z}, R, R_{\Delta}\}. \quad (12)$$

Thus the weights in (7) become $Q = C_p^T Q C_p$, $R = D_p^T Q D_p$, $S = C_p^T Q D_p$. As a rule of thumb, increasing Q_q can damp q overshoot and increase phase margin, but increase rise time. Increasing Q_{n_z} increases rise time. Increasing $Q_{\Delta q}$ increases phase margin, but can also increase rise time. It is more effective than Q_q on this front but does not reduce q overshoot so much. Increasing R slows the response, increases high-frequency roll off and increases gain margin, but can reduce phase margin, slow response and increase overshoot. $Q_{\Delta n_z}$ and R_{Δ} have less pronounced effects. We choose \bar{x}_0 as a vector of zeros with unity on the state corresponding to the previous input (this appeared most reliable at the most challenging (high altitude, high mass, forward CoG) flight points).

The optimisation (9) is expressed using YALMIP (Löfberg, 2004) and solved using MOSEK. In case the problem becomes too ill conditioned, the chosen \bar{x}_0 can be scaled, or the full problem can be scaled by similarity transformation on $\bar{A}(\theta)$ and equivalent scaling on all other matrices. To gain an idea of the best levels of performance that can be achieved, we relegate tuning of (12) to an optimisation-based procedure implemented using the Simulated-Annealing solver, ASA (Ingber, 2012). The chosen cost-function for this tuning minimises a weighted sum of 6 criteria given a 10 s step response for each flight point in a given flight group: $c_1 = \max_i \sum_{k=0}^{k_{\max}} (n_z(k) - y_{ref}(k))^2$, $c_2 = \sum_i \max(0, \max_k (n_z(k) - 1.1))$, $c_3 = \sum_i \max(0, \max_k (q(k)/q_{k_{\max}}) - 1.3)$, $c_4 = \sum_i \max(0, \max_k (-PM + 60))$, and c_6 is the sum over design points θ_{ji} of the maximum gain above the roll-off from -10 to -30 dB between 20 and 78 rad/s evaluated at 1 rad/s intervals. PM, and GM are phase and gain margins in deg and dB, and $y_{ref}(k)$ is the response to a first-order system plus a delay representing the desired ‘‘ideal’’ response. The controller parameters could be tuned directly also in this way, but the proposed method allows for intuitive interactive fine-grained re-tuning based on previously stated rules.

4.1 Airspeed failure

Figure 2 shows the closed-loop step responses of the linearised short-period model (with filters and actuator) over the range of airspeeds at vertices of the $[0, 1]$ -normalised mass/CG envelope at an altitude of 5000 ft. The rise-time to 90% (6 s) and overshoot in q (30%) and n_z (10%) are met, and the response, whilst not as consistent as possible

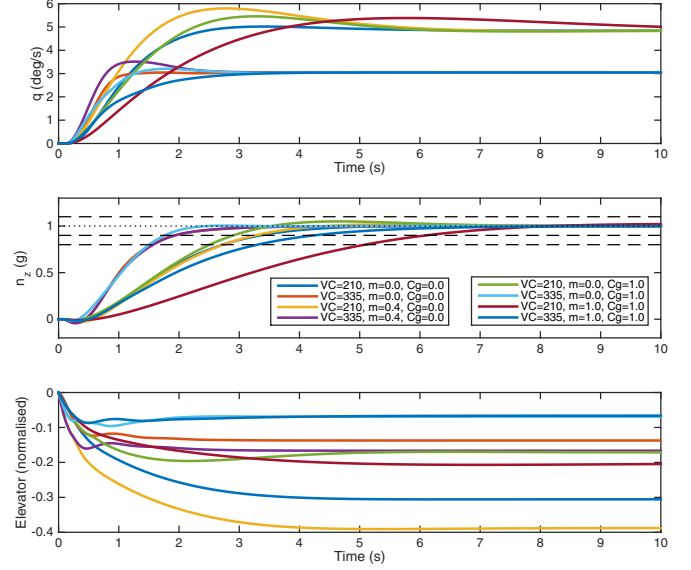


Fig. 2. Step response for linear models at 5000 ft

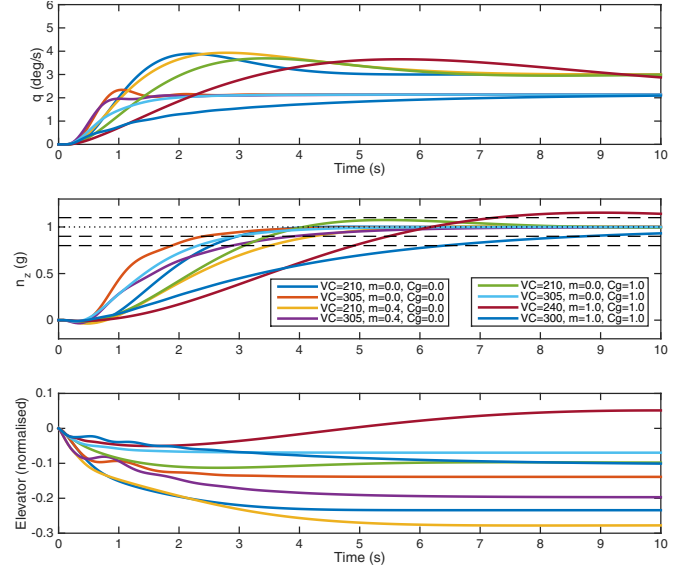


Fig. 3. Step response for linear models at 35000 ft

with a fully scheduled control law varies in a predictable manner. Figure 3 shows the closed-loop step responses over the vertices of the airspeed, mass and CoG envelope at 35000 ft. Most flight points meet the required specifications, except at the highest-mass, most forward CoG, where it is very difficult to simultaneously stabilise the upper and lower airspeeds. Here, there are slight violations of rise time requirement at high airspeed and overshoot at low airspeed. Nevertheless the system is stable.

4.2 Airspeed, mass and CoG missing

When mass and CoG are also polluted a control law can be designed to simultaneously stabilise all vertices of the flight envelope for a given altitude. Figure 4 shows the step response for such a control law at 5000 ft. This has been tuned to achieve at maximum 40% overshoot in q , 10% overshoot in n_z and a linear phase margin of 40° at each of the design points so as to achieve the required n_z response.

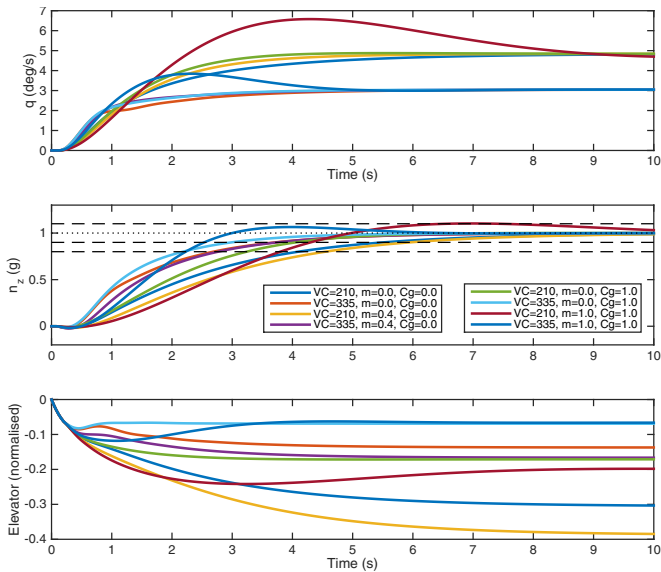


Fig. 4. Step response for linear models at 5000 ft: no mass or CoG

5. NONLINEAR APPLICATION

Figure 6 shows a high-level functional description of the online control task. A simple gain-scheduling (Rugh and Shamma, 2000) approach is employed, with the control gains interpolated based on the non-faulty flightpoint parameters. The control law must also be defined for small deviations outside the nominal flight envelope. Since the grid describing the flight groups is not completely regular, firstly, “fictitious” flight groups are used to “pad” the flight envelope to allow it to be bounded by simple box constraints. This is done by repeating the data for the nearest defined flight point. Then a Delaunay Triangulation is performed. At a given point in the flight envelope, the control gain is obtained by a barycentric interpolation of the gains computed for the simplex containing the current flight parameters. To clarify this, Figure 5 shows the triangulation. Mass and CoG positions are normalised into the range $[0, 1]$ corresponding to the bounds of their admissible values. Green markers indicate the extended padding used to allow use of simple box saturation online. Whilst the point-location and interpolation task is conceptually simple and can be performed using standard MATLAB tools, the online task can be further simplified by re-sampling the interpolation offline (red markers) to partition the padded flight envelope into cuboids. This allows implementation in Simulink using (for the case where mass and CoG are available) a pre-lookup block and an array of “Interpolation Using Prelookup” blocks. The case where only altitude is available is a trivial corollary.

5.1 Airspeed failure

The RECONFIGURE benchmark simulator is a high-fidelity industrially-validated nonlinear simulator provided to the RECONFIGURE consortium by Airbus. It comprises of two parts: a compiled “black box” running on a Linux server, which simulates the flight dynamics; and a Simulink-based interface containing parts of the flight control computer logic with sufficient hooks to allow replacement of the built-in benchmark control law with a custom design.

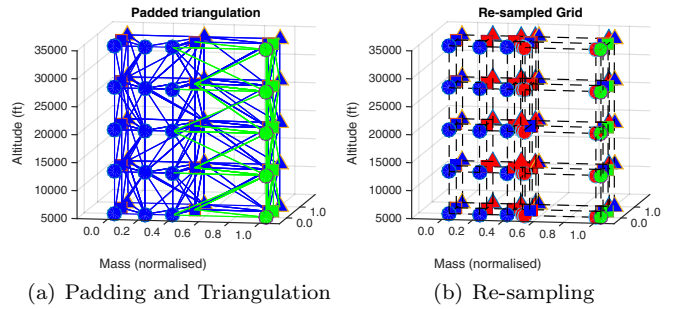


Fig. 5. Flight envelope padding, triangulation and re-sampling (normalised-CoG into the page)

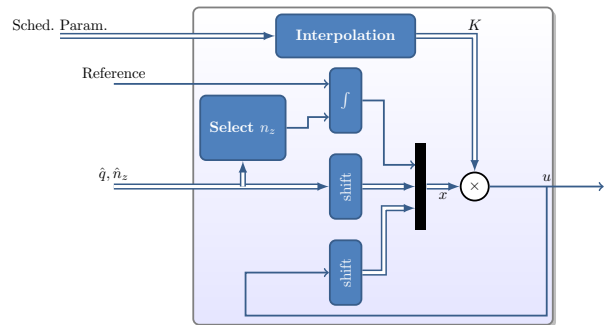


Fig. 6. High-level functional description of implementation

The two parts communicate over a network link using an Airbus proprietary protocol. To demonstrate the behaviour of the proposed control law, the control law is implemented as a Model Reference Block in Simulink and connected in place of the nominal (fully scheduled) benchmark control law. When airspeed measurements are unavailable, but mass and CoG are usable, the design from Section 4.1 is demonstrated, interpolated based on mass, CoG and altitude. Figure 7 shows the closed-loop responses to a sequence of pilot sidestick commands corresponding to a small backward deflection at $t = 5$ s followed by a return to neutral at $t = 16$ s, a small forward deflection at $t = 27$ s and neutral at $t = 38$ s, from a selection of initial conditions. Standard outer “protection” loops and autothrust are disabled since these are polluted by the faults. As well as demonstrating transient behaviour this also shows the response as airspeed varies.

5.2 Airspeed, mass and CoG failure

Figure 8 shows the closed-loop responses in the nonlinear benchmark to the robust control law designed to not depend upon airspeed, CoG or mass estimates at all design points at 5000 ft, i.e. for a given altitude each simulation will use the same control law. Performance is adequate, except for the high-mass, forward CoG and low airspeed scenario, in which due to absence of protection loops and autothrottle the airspeed deviates from the design envelope and the quality of control deteriorates. Elevator responses are more “cautious” than the scenario where CoG and mass are available. The n_z response is more homogeneous for this scenario, perhaps due to design using a common cost function for all CoG/mass/airspeed values, and perhaps due to less stringent additional robustness criteria applied during tuning.

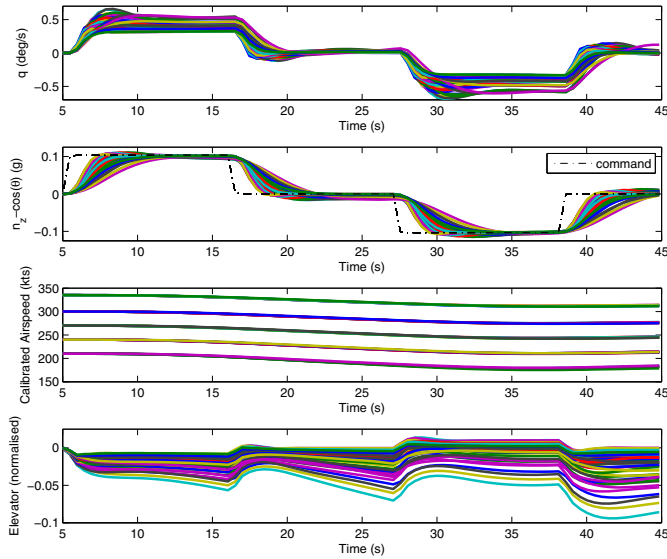


Fig. 7. Closed-loop simulation (no airspeed) in nonlinear RECONFIGURE benchmark: all design points at 5000 ft

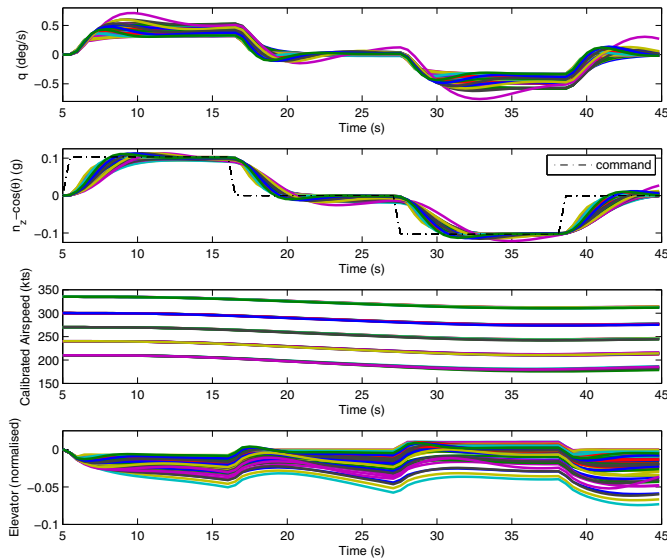


Fig. 8. Closed-loop simulation (altitude only) in nonlinear RECONFIGURE benchmark: all design points at 5000 ft

6. CONCLUSIONS

A robust load-factor tracking control law for the longitudinal dynamics of an aircraft has been proposed and demonstrated in linear and nonlinear simulation. The performance requirements are met over a large region of the flight envelope, and a further degraded control law which does not require even mass or centre of gravity estimates has also been demonstrated. Heavy computation is relegated to the offline design phase, and the online computational task involves only simple operations. Future developments will involve a more rigorous treatment of the behaviour between design points and of implementing a switching and initialisation procedure to allow bumpless transfer from the nominal control law upon detection of the faulty scheduling data, as well as the possibility of application of nonlinear

state estimation or online parameter-identification based control laws to improve performance, or to provide a substitute for the invalidated outer AoA and airspeed protection loops.

REFERENCES

- Brière, D., Favre, C., and Traverse, P. (1995). A family of fault-tolerant systems: electrical flight controls, from Airbus A320/330/340 to future military transport aircraft. *Microprocessors and Microsystems*, 19(2), 75–82.
- Cuzzola, F.A., Geromel, J.C., and Morari, M. (2002). An improved approach for constrained robust model predictive control. *Automatica*, 38(7), 1183–1189.
- de Oliveira, M.C., Bernussou, J., and Geromel, J.C. (1999). A new discrete-time robust stability condition. *Syst. Control Lett.*, 37(4), 261–265.
- De Oliveira, M.C., Geromel, J.C., and Bernussou, J. (2002). Extended H_2 and H_∞ norm characterizations and controller parametrizations for discrete-time systems. *Int. J. Control*, 75(9), 666–679.
- Ding, B. and Zou, T. (2014). A synthesis approach for output feedback robust model predictive control based-on input–output model. *J. Process Contr.*, 24(3), 60–72.
- Favre, C. (1994). Fly-by-wire for commercial aircraft: the airbus experience. *Int. J. Control*, 59(1), 139–157.
- Goupil, P. (2011). AIRBUS state of the art and practices on FDI and FTC in flight control system. *Control Eng. Pract.*, 19(6), 524–539.
- Goupil, P., Boada-Bauxell, J., Marcos, A., Cortet, E., Kerr, M., and Costa, H. (2014). AIRBUS efforts towards advanced real-time fault diagnosis and fault tolerant control. In *Proc. 19th IFAC World Congress*, 3471–3476. Cape Town, South Africa.
- Granado, E., Colmenares, W., Bernussou, J., and Garcia, G. (2005). LMI based robust output feedback MPC. In *Proc. 44th IEEE Conf. Decision and Control, and European Control Conf. (CDC-ECC)*, 5764–5769. Seville.
- Ingber, L. (2012). *Adaptive simulated annealing (ASA) README*. URL <http://www.ingber.com/#ASA>.
- Kothare, M.V., Balakrishnan, V., and Morari, M. (1996). Robust constrained model predictive control using linear matrix inequalities. *Automatica*, 32(10), 1361–1379.
- Löfberg, J. (2004). YALMIP: A toolbox for modeling and optimization in MATLAB. In *Proc. CACSD Conference*. Taipei, Taiwan. URL <http://control.ee.ethz.ch/~jloef/yalmip.php>.
- Maciejowski, J.M. (2002). *Predictive Control with Constraints*. Pearson Education.
- Puyou, G. and Ezerzere, P. (2012). Tolerance of aircraft longitudinal control to the loss of scheduling information: toward a performance oriented approach. In *Proc. 7th IFAC Symp. Robust Control Design*, 393–399. Aalborg, Denmark.
- Rugh, W.J. and Shamma, J.S. (2000). Research on gain scheduling. *Automatica*, 36(10), 1401–1425.
- Varga, A., Ossmann, D., and Joos, H.D. (2014). A fault diagnosis based reconfigurable longitudinal control system for managing loss of air data sensors for a civil aircraft. In *Proc. 19th IFAC World Congress*, 3489–3496. Cape Town, South Africa.
- Wan, Z. and Kothare, M.V. (2002). Robust output feedback model predictive control using off-line linear matrix inequalities. *J. Process Contr.*, 12(7), 763–774.